Research Article

Jing Wang*, Qian Qu, Suleman Ayub Khan, Badr Saad Alotaibi, Fadi Althoey, Yaser Gamil, and Taoufik Najeh*

Experimenting the influence of corncob ash on the mechanical strength of slag-based geopolymer concrete

https://doi.org/10.1515/rams-2023-0187 received October 12, 2023; accepted January 31, 2024

Abstract: The construction sector has been under growing public attention recently as one of the leading causes of climate change and its detrimental effects on local communities. In this regard, geopolymer concrete (GPC) has been proposed as a replacement for conventional concrete. Predicting the concrete's strength before pouring is, therefore, quite useful. The mechanical strength of slag and corncob ash (SCA-GPC), a GPC made from slag and corncob ash, was predicted utilizing multi-expression programming (MEP). Modeling parameters' relative importance was determined using sensitivity analysis. When estimating the compressive, flexural, and split tensile strengths of SCA-GPC with MEP, 0.95, 0.93, and 0.92 R^2 -values were noted between the target and predicted results. The developed models were validated using statistical tests for error and efficiency. The sensitivity analysis revealed that within the mix proportions, the slag quantity (65%), curing age (25%), and fine

aggregate (3.30%) quantity significantly influenced the mechanical strength of SCA–GPC. The MEP models result in distinct empirical equations for the strength characteristics of SCA–GPC, unlike Python-based models, which might aid industry and researchers worldwide in determining optimal mix design proportions, thus eliminating unneeded test repetitions in the laboratory.

Keywords: geopolymer concrete, corncob ash, mechanical strength

1 Introduction

Over time, the environmental impact of concrete's lengthy history as a key construction material has come into focus [1]. The global demand for cement and concrete is predicted to triple by 2050, which will increase carbon emissions and hasten the loss of biodiversity [2]. Researchers have been trying to develop new binders to replace Portland cement (PC) because of its high energy and carbon footprint [2]. The primary binding component in concrete, PC, is made using around 1.7 tons of raw ingredients and 0.8 tons of carbon dioxide [3]. In light of this, immediate action is necessary to mitigate the effect of cement production on climate change [2]. Scientific and technological advancements have made it possible to recycle agricultural and industrial waste into new construction materials, which contributes to material sustainability [4–6]. Supplementary cementitious materials made from recycled agricultural and industrial waste have positive effects on the environment, the economy, and society as a whole [7–9]. Substituting reused products for PC is an effective, cost-effective, and sustainable way to lessen one's impact on the environment [10-12].

An eco-friendly alternative to traditional concrete, geopolymer concrete (GPC) uses recycled agricultural and industrial materials in place of cement as a binder [13–15]. Geopolymerization indicates that the utilization of alkali silicate/alkali

Qian Qu: School of Civil Engineering, Chongqing Industry Polytechnic College, No.1000 Taoyuan Avenue, Airport, Yubei District, Chongqing 401120, China

Suleman Ayub Khan: Department of Civil Engineering, COMSATS University Islamabad, Abbottabad 22060, Pakistan

Badr Saad Alotaibi: Architectural Engineering Department, College of Engineering, Najran University, Najran, Saudi Arabia

Fadi Althoey: Department of Civil Engineering, College of Engineering, Najran University, Najran, Saudi Arabia

Yaser Gamil: Department of Civil Engineering, School of Engineering, Monash University Malaysia, Jalan Lagoon Selatan, 47500 Bandar Sunway, Selangor, Malaysia

^{*} Corresponding author: Jing Wang, School of Civil Engineering, Chongqing Industry Polytechnic College, No.1000 Taoyuan Avenue, Airport, Yubei District, Chongqing 401120, China, e-mail: wangjing_913@163.com

^{*} Corresponding author: Taoufik Najeh, Operation and Maintenance, Operation, Maintenance and Acoustics, Department of Civil, Environmental and Natural Resources Engineering, Lulea University of Technology, Lulea, Sweden, e-mail: taoufik.najeh@ltu.se

hydroxide is involved in the initiation of raw materials grounded on aluminosilicate [16]. Aluminate and silicate species are released as a result of the source materials' dissolution and de-polymerization during this process. The species undergo reorganization and polymerization, eventually creating a network of geopolymer in three dimensions. As time passes, the resultant gel hardens, adding to the material's durability [17]. Fly ash (FAS), silica fume, metakaolin (MK), red mud, ground granulated blast furnace slag (GGBFS), and rice husk ash (RHA) are only a few of the many examples of recycled agricultural and industrial materials that show promise as geopolymer (aluminosilicate) precursors [18–27]. As an alternative to GPC, GGBFS's reasonable cost-benefit and low environmental impact make it a promising component of eco-friendly and cost-effective concrete [28,29], augmented stiffness [30], and great opposition to chemical attacks [31,32]. However, CCA is a relatively new ingredient. Due to its increased silica concentration, CCA can be used in place of or in addition to traditional pozzolanic materials such as FAS and RHA. Sustainable infrastructure projects use geopolymer-stabilized road bases [33]. This technology increases road strength and durability, minimizing maintenance and increasing lifespan [34]. Geopolymer technology is widely used to build strong, eco-friendly transportation networks. Researchers are looking toward making this green concrete at room temperature in order to avoid the problems associated with using GPC that have been baked in an oven on-site. Understanding that meeting strength standards is not the only criterion for evaluating performance is also crucial. Resistance to environmental and other pressures should be considered when estimating a building's service life. One possible alternative to traditional concrete for environmentally sensitive places is GPC, which provides longer life and stronger mechanical characteristics [31]. The aforesaid sources all agree that GPC's superior durability and mechanical capabilities can be attributed to the material's distinct chemical composition [23,35,36]. In recent years, GPC's performance has increased because of the use of nano-silica and recycled plastic particles [37–39].

Engineers, scientists, researchers, and computer programmers are finding that artificial intelligence (AI) greatly influences their work in developing new products and

improving existing ones. Researchers who are able to apply AI to their regular work are in high demand to answer a wide range of difficulties facing the engineering industry. Despite the promising future of AI-based systems, several drawbacks and performance worries remain. They had a hard time with things that humans take for granted, such as recognizing objects and following conversations [40]. Because of this, current AI has a hard time coming up with adequate alternatives for teaching computer intuition. Machine learning (ML) has been employed by AI systems as a means of addressing these concerns [40,41]. ML algorithms allow computers to acquire the knowledge they need to perform an action by inspecting a sufficiently big data collection [42,43]. Prior to implementing the strategy, it is necessary to reclaim the characteristics that best characterize the most precise data. The phrase "feature extraction" is used to characterize this technique. Then, the sample data, attributes, and pattern separation instructions are trained using ML [40,44,45]. Modern research in civil engineering must incorporate statistical methods and AIAI to tackle increasingly complex challenges. One popular use of AI and statistical approaches in civil engineering is to forecast concrete's compressive strength (CS) [1,20,46,47]. Some of the more challenging problems that have been addressed with these methods include the prediction of chloride penetration, the shear behavior of beams, the axial behavior of various columns, and the strength and slump of self-compacting concrete [48-51]. Future studies can benefit from these predictions since they limit the number of potential test configurations, which in turn makes them shorter and cheaper. Many ML methods, such as gene expression programmings (GEPs), artificial neural networks (ANNs), decision trees (DTs), boosting, gaussian process regressions, regression trees, expression trees, support vector machines (SVMs), and MEPs, can be used to predict concrete strength [52–54]. The mechanical properties were forecasted employing the MEP approach, which is one of the highly accurate ML methods. Prior ML-based relevant research work is provided in Table 1.

In this study, the mechanical strength of GPC made from slag and corncob ash (SCA–GPC) was predicted using AI techniques based on experimental results. The objectives of

Table 1: ML-based literature study

Ref.	Materials studied	Properties predicted	ML method employed
[55]	Fiber-reinforced concrete	Ultrasonic pulse velocity	Gradient boosting extreme gradient boosting.
[56]	ordinary portland cement–concrete	CS	SVM and ANN
[57]	Wood ash-cement-nano TiO ₂ -based mortar	Mechanical properties	ANN
[58]	Phosphoric acid slurry	Dynamic viscosity	ANN, DT, and random forest (RF)
[59]	Lightweight geopolymer mortar	CS	GEP
[60]	MK-based concrete	Mechanical properties	GEP and MEP

Table 2: Statistical accounts of a set of factors

Descriptive statistics BFS (kg·m ⁻³) CCA (kg·m ⁻³) FA (kg·m ⁻³)	BFS (kg·m ⁻³)	CCA (kg·m ^{−3})	FA (kg·m ^{−3})	CA (kg·m ⁻³)	<i>W</i> (kg·m ⁻³)	SHP (kg·m ⁻³)	SSG (kg·m ⁻³)	CD (days)	MC (M)	CG (MPa)	CS (MPa)	FS (MPa)	STS (MPa)
Mean	218.65	215.24	818.12	1044.99	35.22	23.38	146.40	45.25	14.00	34.96	35.90	5.36	3.65
Standard error	9.54	9.48	3.53	0.01	0.13	0.13	0.00	1.93	0.10	0.31	92.0	90.0	0.04
Median	228.00	195.00	841.00	1045.00	35.16	23.44	146.40	42.00	14.00	30.00	36.04	5.47	3.60
Mode	0.00	0.00	841.00	1045.00	37.86	20.74	146.40	7.00	12.00	30.00	29.04	2.00	3.60
Standard deviation	153.90	152.78	56.90	60.0	2.15	2.15	0.01	31.20	1.65	5.01	12.19	1.01	99.0
Sample variance	23685.6	23341.7	3237.34	0.01	4.63	4.63	0.00	973.43	2.72	25.10	148.64	1.03	0.43
Kurtosis	-1.12	-1.12	-1.41	127.47	-1.53	-1.53	127.47	-1.34	-1.53	-2.02	-0.74	-0.58	0.58
Skewness	0.12	0.13	-0.14	-1.34	0.04	-0.04	-1.34	0.25	0.00	0.02	0.17	-0.24	0.20
Range	488.00	488.00	171.00	1.00	5.22	5.22	0.10	83.00	4.00	10.00	53.42	4.64	4.57
Minimum	0.00	0.00	728.00	1044.00	32.64	20.74	146.30	7.00	12.00	30.00	10.67	2.81	1.97
Maximum	488.00	488.00	00.668	1045.00	37.86	25.96	146.40	90.00	16.00	40.00	64.09	7.45	6.54
Sum	56850.0	55962.0	212712.0	271698.0	9157.44	6078.5	38063.8	11765.0	3640.0	0.0606	9334.0	1393.58	949.4

the study were achieved by employing the multi-expression programming (MEP) method. The MEP approach was opted for because it provides empirical equation-based models that can be implemented worldwide in potential future mix design formulations. Running statistical tests and comparing the modeled and observed results allowed for an assessment of the models' approximative correctness. Experiments are labor and resource-intensive because of the complexities inherent in their techniques as they involve obtaining the required materials, casting the samples, curing them to increase their strength, and finally evaluating them. Applying state-of-theart modeling techniques, such as ML, to the building industry could substantially aid in mitigating these issues. The combined impact of the many parameters on SCA-GPC strength is very difficult to detect using conventional testing methods. In this study, sensitivity analysis was employed to look at the relative significance of different variables. The information that ML techniques need can be gathered from previous studies. That means that the dataset can be utilized in ML procedure runs, estimates of material properties, and investigations of impacts. The effectiveness of the MEP method for forecasting SCA-GPC strength was verified in this article by using an experimental dataset. The outcomes of this study have the potential to influence sustainable building methods and increase GPC's adaptability in the construction industry.

2 Investigation methods

2.1 Gathering data and evaluation

This study sought to forecast the CS, flexural strength (FS), and split-tensile strength (STS) of SCA-GPC, a GPC made from slag and corncob ash (CCA), using MEP models [47]. A grand total of 260 data points were produced by the experimental investigation. The anticipated STS, FS, and CS of SCA-GPC were established on the following 10 input factors: CCA, molar concentration (MC), fine aggregate (FA), blast furnace slag (BFS), sodium hydroxide pellets (SHP), coarse aggregate (CA), curing day (CD), sodium silicate gel (SSG), water (W), and concrete grade (CG). In order to gather and arrange the data, data preparation was employed. It is common practice to employ data preparation for data mining in order to circumvent a major roadblock while attempting the recognized method of information finding from data. Cleaning the data of noise and unnecessary details is what data preparation is all about. The outcomes of numerous descriptive statistics that were computed with these data are presented in Table 2. The accuracy of the models used was also evaluated through validation. The

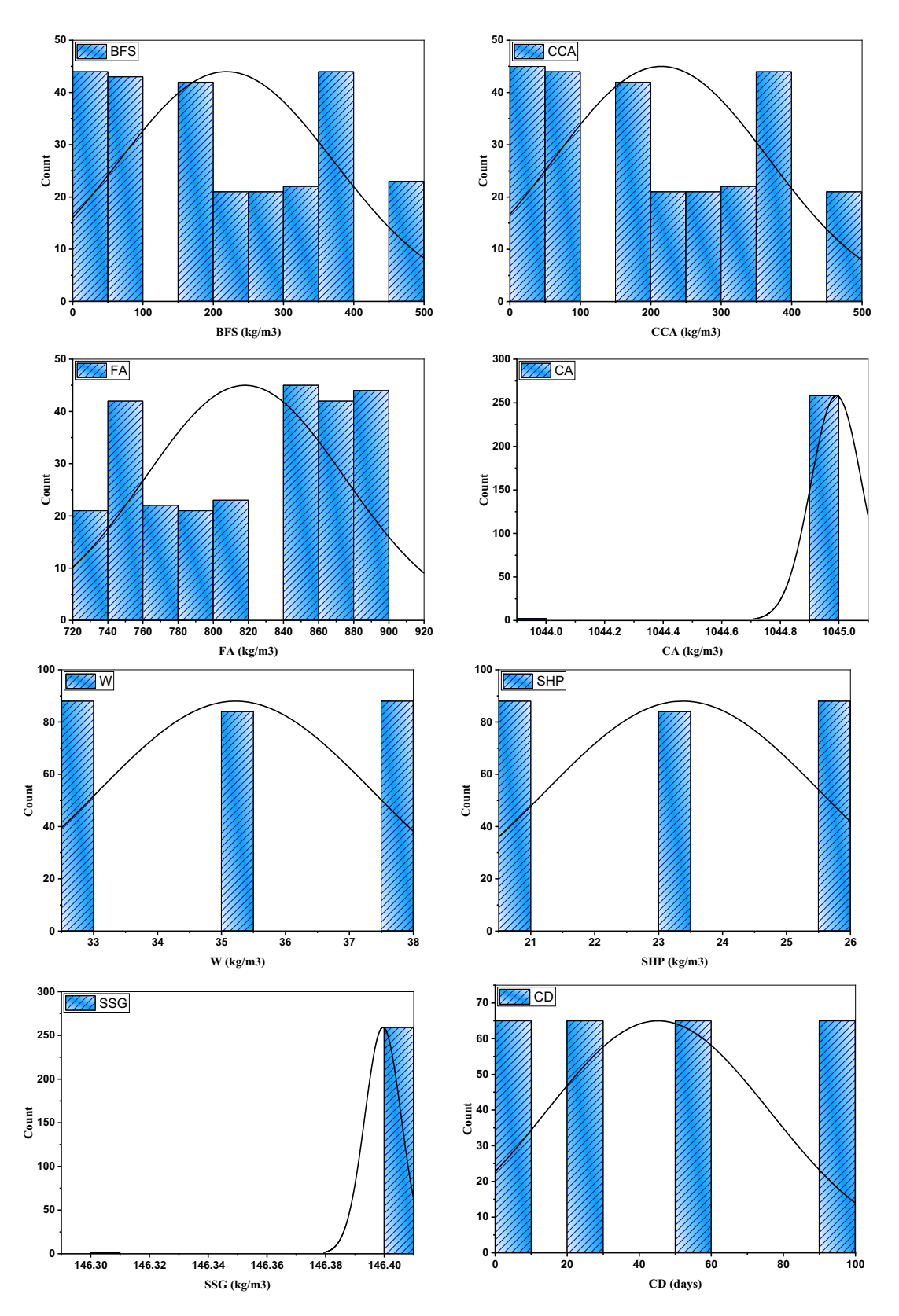


Figure 1: Statistical dissemination of dataset parameters.

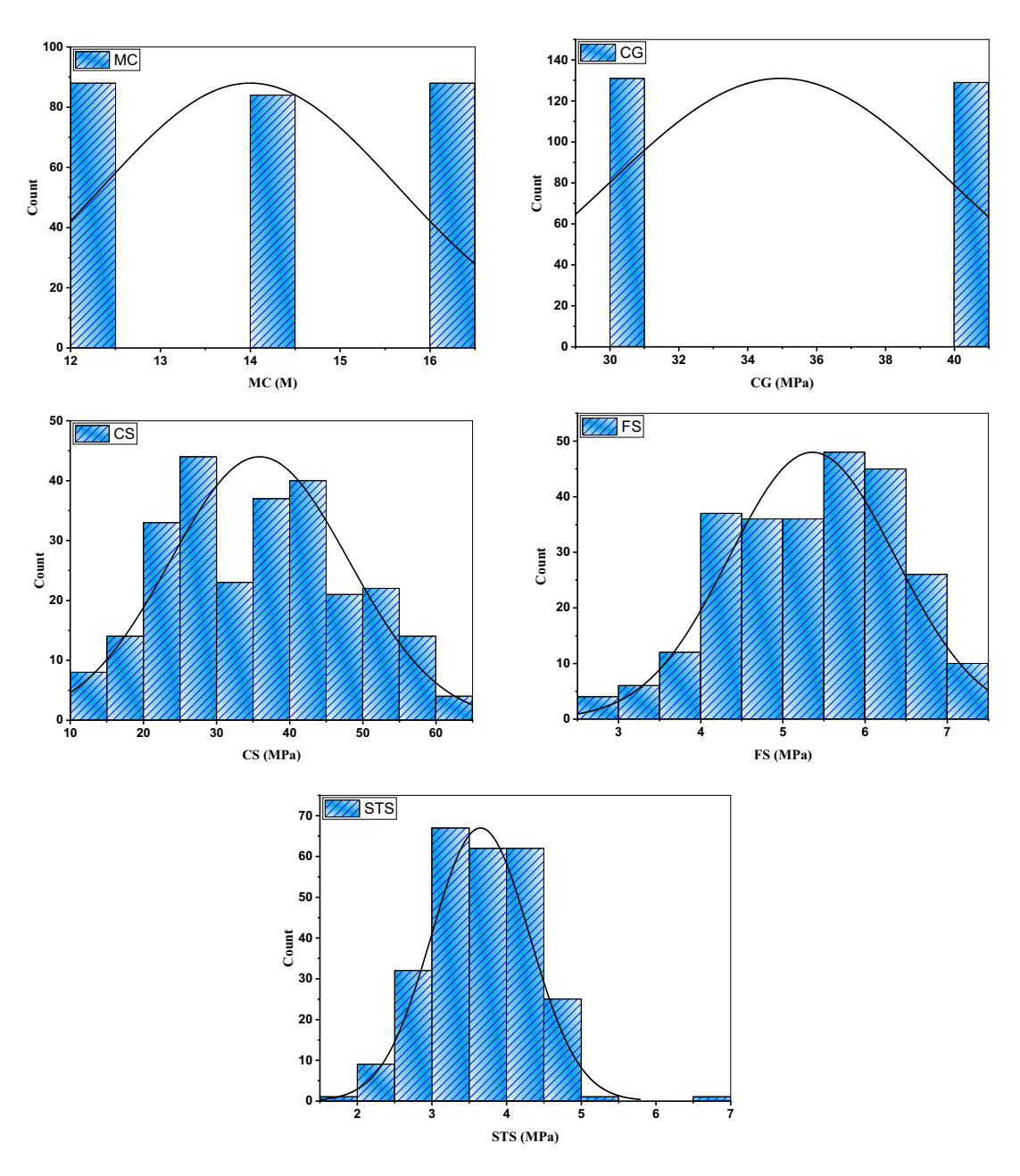


Figure 1: (Continued)

graphs in Figure 1 demonstrate the distributions of the values' frequencies. Just by adding together the distributions of all the pieces of a dataset, you may determine its overall frequency distribution. By creating a relative frequency distribution, one may observe the frequency with which particular values occur.

Input data distribution and patterns are known to affect the prediction model. Figure 1 shows the resulting distribution of frequencies of the supplied dataset. The graph below shows that the input data frequencies are relatively high, and the distribution is not uniform, suggesting that the models can be used for more varied data. In addition, Table 2 provides a variety of statistical values for data to shed light on the database. These tables display information about the input data, such as its distribution (standard deviation and variance), mean, extreme, and pattern (kurtosis and skewness). Skewness was used to check the symmetry of the data, and everything was fine there because all the research variables were within the optimal range of 3 to +3. A measure of the distribution's peakedness or flatness called kurtosis was also employed [61]. All of the model variables' kurtosis values fell within the acceptable range

6 — Jing Wang et al. DE GRUYTER

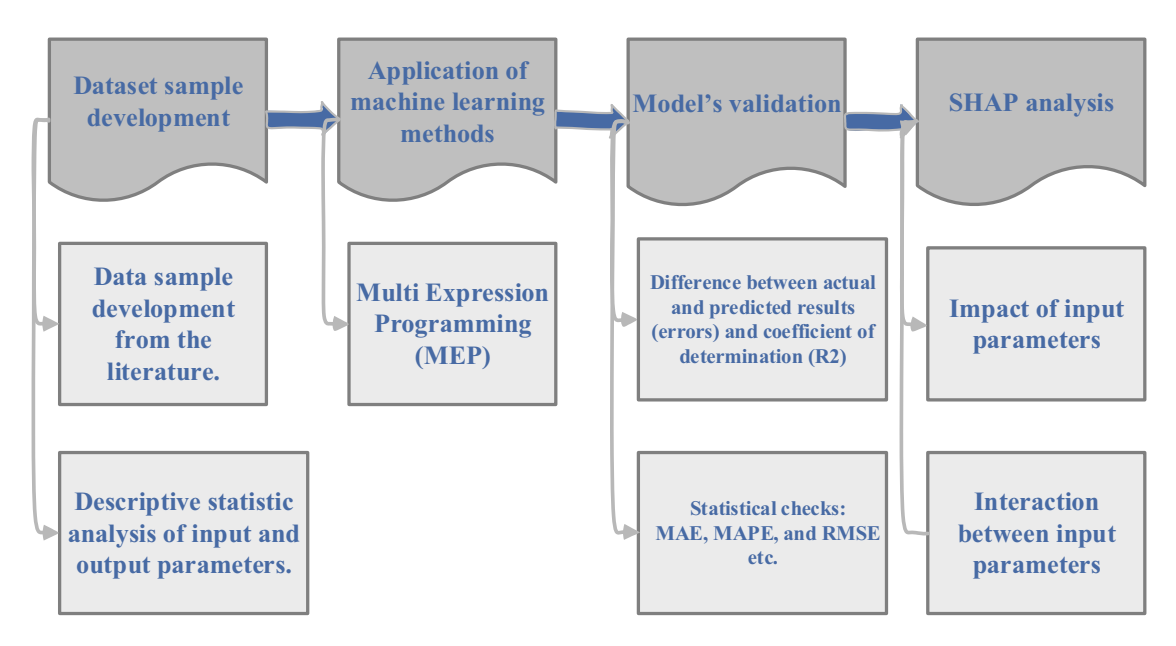


Figure 2: Diagram for a ML-based investigation.

of 10 to +10, indicating a well-shaped distribution and avoiding drastic outliers [62,63].

2.2 ML simulations

In a controlled laboratory setting, the mechanical characteristics of SCA-GPC were investigated. The production of STS, FS, and CS requires the incorporation of ten distinct ingredients. A cutting-edge ML technique called MEP was used to forecast the SCA-GPC's STS, FS, and CS. The primary use case for ML algorithms is the comparison of outputs to inputs. 70% percent of the data was utilized to train ML models, whereas just 30% of it was used for testing. In order to train the model to learn patterns on most of the data and then assess its generalization performance on an independent set, the data split is a crucial step in evaluating ML models. To avoid over-fitting to the training set and get a good idea of the model's predictive skills, this split is useful for testing how it does on unknown data. A similar data-splitting approach has been adopted by other scholars in comparable nature studies [64–66]. The R^2 score of the predicted result demonstrated the reliability of the model. The R^2 number indicates how well the actual results match the predictions; a low value indicates a large mismatch [67]. The accuracy of the model was confirmed by multiple analyses, including statistical analyses and error checks. Figure 2 shows a streamlined illustration of an event model. Table 3 displays the values of the hyper-parameters used by the MEP model. The selection of a fitness function, the representation of

programs as linear chromosomes, and the use of evolutionary operators, including mutation, crossover, and selection, are all important requirements in MEP. Important parameters that affect the model are the length of the algorithm or code and the number of subpopulations. The model's capacity to grasp complex relationships in the data is influenced by the complexity and expressive power of the evolved programs, which are, in turn, affected by the number of subpopulations and the diversity of the population, both of which affect the exploration—exploitation trade-offs.

Symbolic mathematical expressions are generated by MEP, an evolutionary computation technique, in the

Table 3: Details for MEP models defined

MEP				
Factors	Settings			
Terminal set	Problem input			
Number of generations	500			
Problem type	Regression			
Number of treads	2			
Number of runs	15			
Function set	Square root, $+$, $-$, \times , \div			
Error	MSE, MAE			
Mutation probability	0.01			
Subpopulation size	100			
Replication number	15			
Code length	50			
Number of subpopulations	50			
Operators/variables	0.5			
Crossover probability	0.9			

context of GPC mechanical property prediction. Finding the optimal program to describe the link between input parameters and CS is the goal of MEP, which is accomplished through an iterative process of creating mathematical programs within a population. There are evolutionary operators that direct population refinement and a fitness function that assesses how well each program approximates observations of mechanical property values. Using the input parameters, the MEP-generated model predicts the mechanical properties of GPC by extracting the bestperforming mathematical expression. The size and complexity of MEP mathematical expressions depend on code length. Longer codes allow more complex expressions, which may capture data relationships. Table 3 lists the parameters, including generations, population size, subpopulations, and code length set for optimized MEP models. They affect the algorithm's capacity to evolve correct math-

ematical representations of mechanical features.

2.2.1 MEP model

DE GRUYTER

The MEP is a state-of-the-art, demonstrative linear-based GP method because of its usage of linear chromosomes. Differentiating MEP from other, more recent variants of the GP method is its ability to encode numerous bits of software (alternatives) into a single chromosome. The result is reached by employing fitness analysis to pick the optimal chromosome [68,69]. According to Oltean and Grosan, this happens when a bipolar system recombines to form two new offspring, with each offspring choosing one parent [70]. As shown in Figure 3, the procedure will continue until the optimal program is found prior to the termination condition. Fitness analysis is crucial in MEP for evaluating evolved mathematical expressions for dataset fitting. The fitness function determines the best chromosomes for reproduction by measuring the difference between a program's output and its target outputs. MEP favors fit programs through selection, crossover, and mutation. Iteratively, the algorithm stops when it reaches a fitness level, a number of generations, or limited improvement, guaranteeing it stops within restrictions. Mutations in MEP arise during evolution and modify linear chromosomal elements. Small chromosomal program mutations increase genetic diversity in the population. Mutations begin early in the MEP optimization process, enabling for unique solutions and impacting future generations' genetic material. Mutations improve the algorithm's solution space search and fitness landscape adaptation. Similar to the other ML paradigms, the MEP model allows for the combination of different parts. In MEP, some of the criteria that matter include the number of subpopulations, the

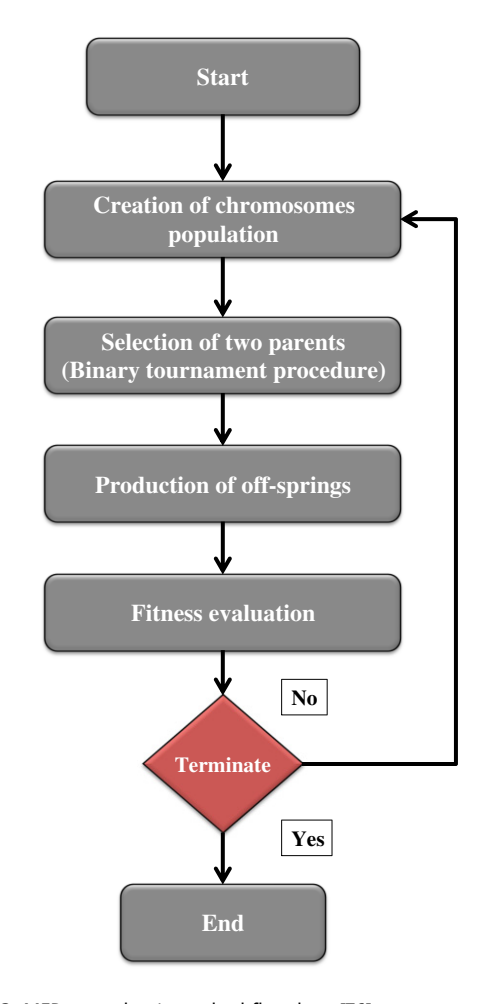


Figure 3: MEP procedure's method flowchart [76].

length of the algorithm/code, the probability of crossover, and the number of functions [71]. Assessing the population becomes more challenging and time-consuming when the population size is the whole number of packages. Also significantly impacted by code length is the size of the produced mathematical expressions. See Table 3 for the full list of MEP parameters needed to build a trustworthy rheological property model.

Using literature datasets is commonplace in the MEP method's evaluation and modeling stages [72,73]. Popular linear GP methodologies like the MEP are deemed by some scholars to be superior for predicting the properties of viable concrete. Linear genomic programming, in conjunction with maximum-likelihood estimation, was determined by Grosan and Abraham to be the most effective neural network-based strategy [74]. The GEP's method of operation is marginally more intricate than that of the MEP [71]. Notwithstanding MEP's reduced density compared to GEP, there are a few key differences: (i) MEP explicitly encodes function argument references; (ii) non-coding components are not required to be exhibited at a set point contained by

the chromosomes; and (iii) MEP allows code re-process [75]. The signs located at the "tail" and "head" of a normal GEP gene make it easy to write syntactically accurate software programs, which leads many to believe that the GEP has superior capabilities [70]. This necessitates a more thorough evaluation of each of these genetic approaches to engineering challenges.

2.3 Authentication of MEP simulations

Models constructed using MEP were tested for statistical validity against a test dataset. The three outputs were evaluated employing (7) distinct statistical techniques [73,77–80]: Nash–Sutcliffe efficiency (NSE), root mean square error (RMSE), mean absolute error (MAE), relative root mean square error (RRMSE), relative squared error (RSE), mean absolute percentage error (MAPE), and Pearson's correlation coefficient (*R*). Eqs. (1)–(7) provide the formulas for various statistical metrics:

$$R = \frac{\sum_{i=1}^{n} (a_i - \bar{a}_i)(p_i - \bar{p}_i)}{\sqrt{\sum_{i=1}^{n} (a_i - \bar{a}_i)^2} \sum_{i=1}^{n} (p_i - \bar{p}_i)^2},$$
 (1)

MAE =
$$\frac{1}{n} \sum_{i=1}^{n} |P_i - T_i|,$$
 (2)

$$RMSE = \sqrt{\sum \frac{(P_i - T_i)^2}{n}},$$
 (3)

MAPE =
$$\frac{100\%}{n} \sum_{i=1}^{n} \frac{|P_i - T_i|}{T_i}$$
, (4)

RSE =
$$\frac{\sum_{i=1}^{n} (a_i - p_i)^2}{\sum_{i=1}^{n} (\bar{a} - a_i)^2},$$
 (5)

NSE = 1 -
$$\frac{\sum_{i=1}^{n} (a_i - p_i)^2}{\sum_{i=1}^{n} (a_i - \bar{p}_i)^2}$$
, (6)

RRMSE =
$$\frac{1}{|\bar{a}|} \sqrt{\frac{\sum_{i=1}^{n} (a_i - p_i)^2}{n}}$$
, (7)

where n is the whole set of numerical values; a_i and p_i are the ith actual and predicted values, correspondingly; and a_i and p_i are the average actual and predicted values, respectively. Usually, the correlation coefficient (R) is used to quantify the prediction power of a model. The correlation between observed and predicted output quantities is high when R is greater than 0.8 [81]. Component R's value, however, remains unchanged when multiplied or divided. R^2 gives a better approximation of the real value since it was computed between the predicted and observed outcomes.

The values of R^2 that are closer to 1 indicate that the model was more effectively built [82,83]. Both MAE and RMSE fared exceptionally well when confronted with progressively more severe mistakes. MAE is the average absolute difference between anticipated and actual values, while RMSE squares these differences, weighting bigger errors. MAE is more effective when big mistakes are not punished, but RMSE is more susceptible to outliers due to the squaring effect. They show how error size affects model performance: greater errors increase RMSE, making it ideal for scenarios where minimizing large errors is critical. When errors are few, the constructed model works better, and the mean absolute error and RMSE get close to zero [84,85]. The most effective datasets for MAE, according to subsequent research, are continuous and smooth [86]. Typically, the model's performance improves as the values of the previous errors decrease.

3 Results and appraisal

3.1 MEP models

3.1.1 CS MEP model

The evolutionary process of MEP yields the empirical formula for GPC CS calculation. The program investigates mathematical expressions involving GPC's ten components such as material kind and proportion. MEP optimizes coefficients and constituent connections to forecast CS using a symbolic formula that best fits the data. To improve the formula, fitness evaluation, selection, crossover, and mutation are used. The empirical formula is a mathematical model of the complicated concrete constituent-CS relationship. The following equation represents the final model equation:

$$CS(MPa) = BFS - \frac{2BFS}{CD} - \frac{2\left(BFS - \frac{BFS}{CD}\right) + MC}{CD} + CG + \frac{CG}{\sqrt{CD}}$$

$$-\frac{CCA - 2BFS + \frac{4BFS}{CD}}{\sqrt{2\left(BFS - \frac{SSG}{CD}\right) + CCA}\sqrt{2\left(BFS - \frac{BFS}{CD}\right) + CCA}}$$

$$+\frac{CD(4FA - \frac{4BFS}{CD} + 2CA)}{(CD - SHP)(CD^2 - 2W + \frac{2SSG}{CD} + CCA)}, \tag{8}$$

where CCA represents corncob ash, SSG represents the Na₂SiO₃ gel, BFS represents the blast furnace slag, W

represents the water; SHP denotes the NaOH pellets, CG represents the concrete grade, CA represents the coarse aggregate, CD denotes the curing day, MC represents the molar concentration, and FA denotes the fine aggregate.

In addition to successfully handling oversimplification, the MEP model exhibits good performance on new, untested data, as seen in Figure 4(a). Well-trained MEP models have learned complex data linkages to capture problem nuances.

The model must prevent overfitting and generalize well to new data, but it must also handle oversimplification. This balance shows the MEP model's ability to handle complexity without becoming too complicated to anticipate real-world outcomes. This model has an R^2 value of 0.956. The CS-MEP model predicts the CS of SCA–GPC more accurately, which is why it has a higher R^2 value. Figure 4(b) shows the results of some MEP simulations that look at the absolute discrepancies

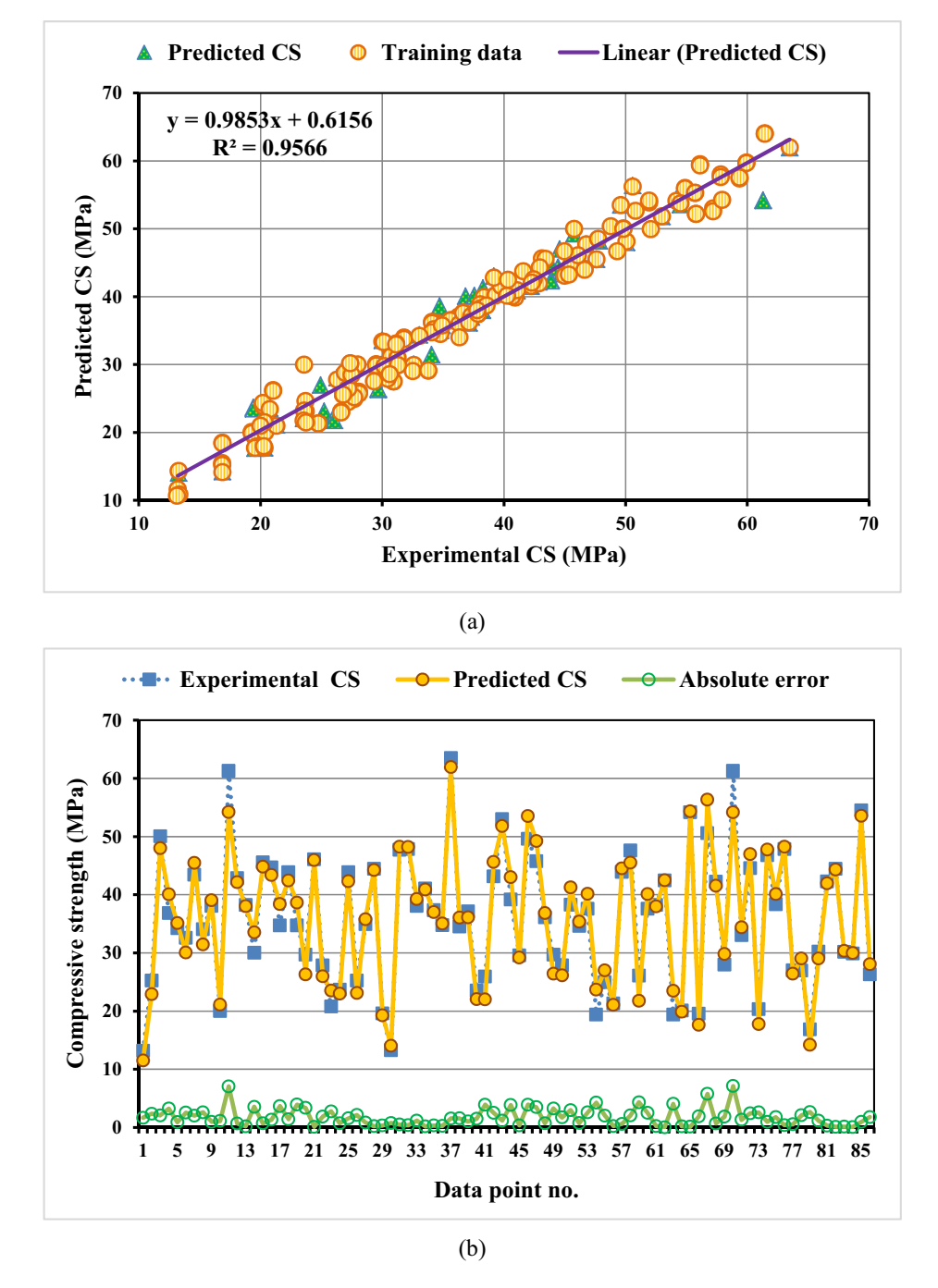


Figure 4: CS-MEP model in SCA-GPC: (a) the relationship between assessed and predicted CS and (b) the dispersion of errors in assessed and forecasted CS.

between the actual and ideal values. Examining absolute differences shows how significantly MEP forecasts diverge from actual values on average. A smaller absolute difference indicates a more accurate forecast, whereas greater discrepancies indicate a wider error range, demonstrating the MEP model's dispersion and reliability. Based on the information provided, the MEP forecast error might be anywhere from 0.04 to 7.13 MPa. In addition, the standard deviation of the errors

was less than 1.79 MPa, with 34 of the readings being less than 1 MPa, 36 being between 1 and 3 MPa, and 16 being greater than 3 MPa. Using the MEP equation reduces the error standard deviations and the degree of correlation (R^2). The MEP equation is often used because of its simplicity and versatility. It would appear that the MEP model is among the best ML prediction models due to its high correlation coefficient and low error rates.

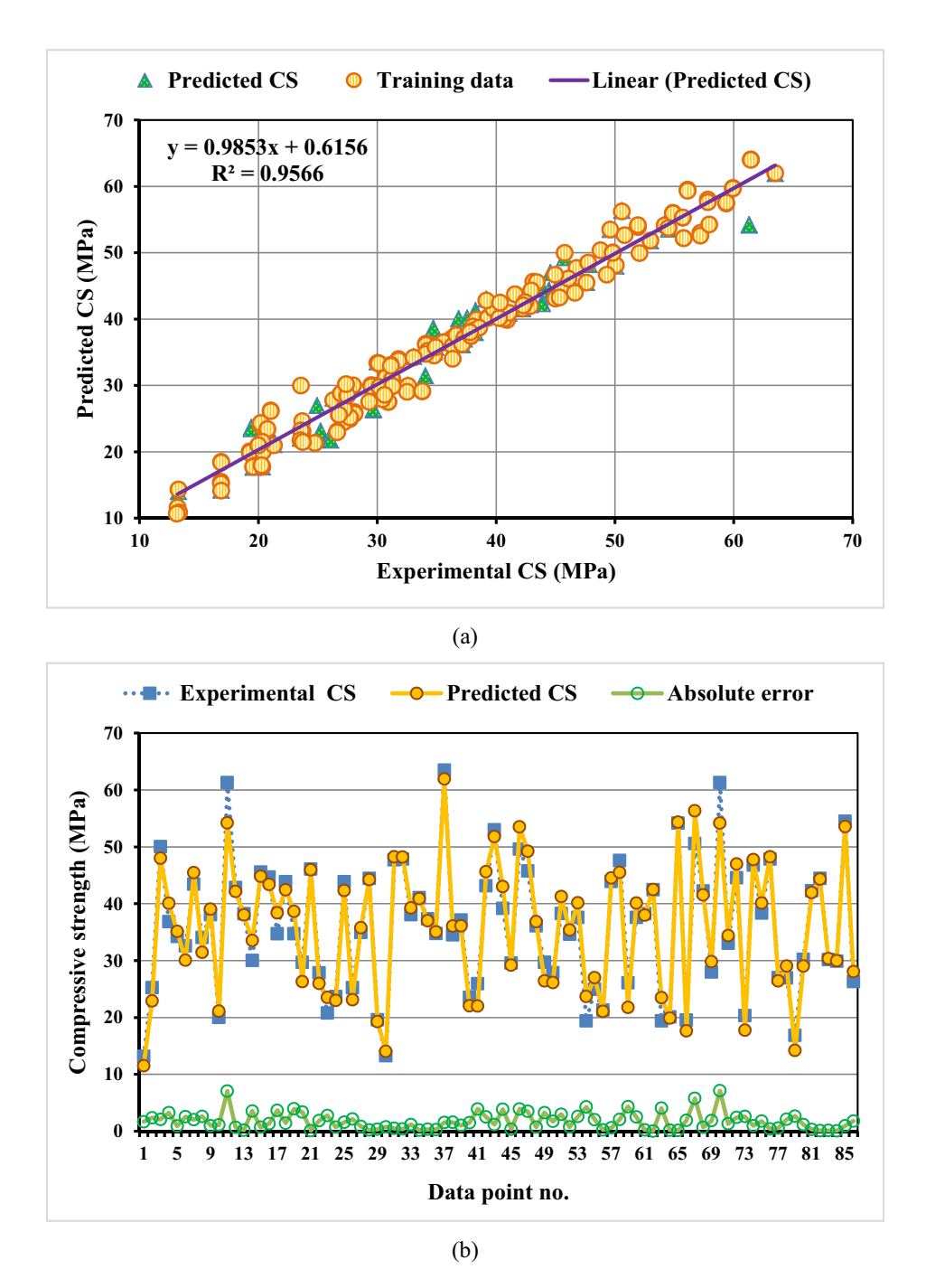
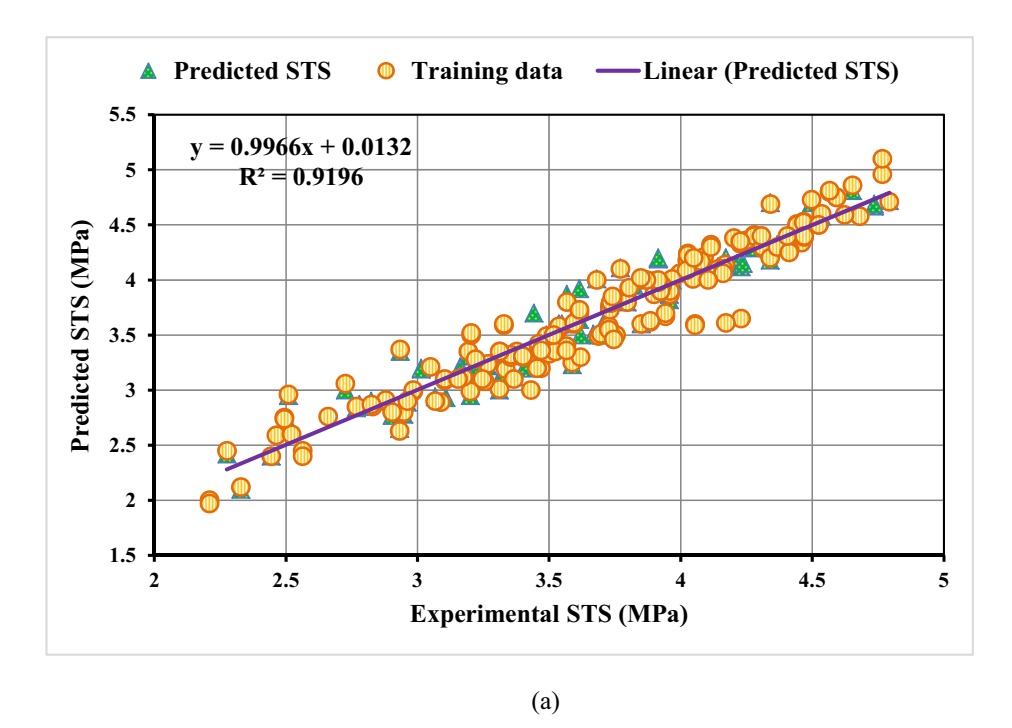


Figure 5: FS-MEP model in SCA-GPC: (a) the relationship between assessed and predicted FS and (b) the dispersion of errors in assessed and forecasted FS.

3.1.2 FS MEP model

The empirical formula for GPC FS calculation comes from MEP evolution. This application examines mathematical formulas involving GPC's ten components, including material kind and proportion. For FS prediction, MEP optimizes

coefficients and constituent links using a symbolic formula that matches data. Fitness evaluation, selection, crossover, and mutation improve the formula. The complex concrete constituent—FS relationship is mathematically modeled by the empirical formula. The following equation displays the final model equations:



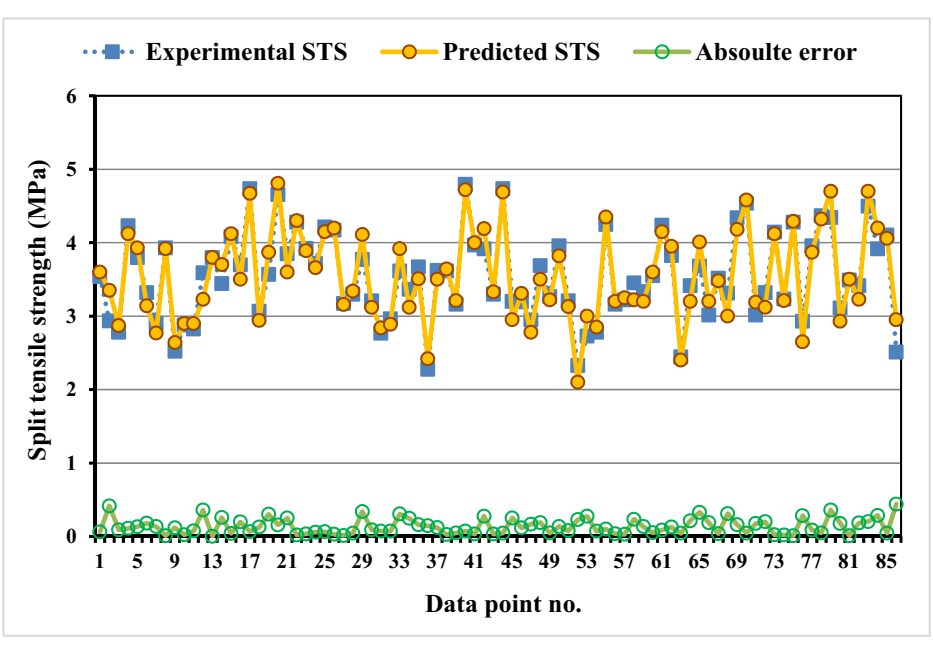


Figure 6: STS-MEP model in SCA-GPC: (a) the relationship between assessed and predicted STS and (b) the dispersion of errors in assessed and forecasted STS.

(b)

$$FS(MPa) = \frac{2FA + \frac{SSG}{MC}}{CA - SSG} - \frac{W}{2CD + \frac{SSG}{MC}} + \sqrt{SHP - \frac{CCA - BFS}{CG}}$$
(9)

where CCA represents the corncob ash, SSG represents the Na_2SiO_3 gel, BFS represents the blast furnace slag, W represents the water, SHP represents the NaOH pellets, CG represents the concrete grade, CA represents the coarse aggregate, CD denotes the curing day, MC denotes the molar concentration, and FA denotes the fine aggregate.

As seen in Figure 5(a), the MEP model handles oversimplification and fresh, untested data well. Well-trained MEP models capture problem nuances with extensive data linkages. While preventing over-fitting and generalizing to new data, the model must also handle oversimplification. This balance indicates the MEP model's capacity to handle complexity without making it too difficult to predict realworld outcomes. The model's R^2 value is 0.932. The FS-MEP model, like the CS-MEP model, has a high R^2 value, which means it predicts the FS of SCA-GPC guite accurately. The utter inconsistencies between the goal and observed values are inspected and shown in Figure 5(b) using MEP simulations. The absolute differences show how far MEP predictions deviate from actual values on average. The MEP model's predictions are dispersed and reliable, with smaller absolute differences indicating a more accurate forecast and larger differences indicating a wider error range. Based on the data provided, the predicted MEP values fell somewhere between 0.0016 and 0.710 MPa. Moreover, the average error value was less than 0.199 MPa due to the following: 23 readings below 0.1 MPa, 43 values between 0.1 and 0.3 MPa, and 20 values beyond 0.3 MPa. Both the CS and FS models' standard deviations of errors and coefficient of correlation (R^2) were significantly reduced when the MEP equations were used.

3.1.3 STS MEP model

MEP evolution produces the empirical formula for GPC STS calculation. The tool examines GPC's ten components, including material kind and proportion, in mathematical terms. A datafitting symbolic formula optimizes coefficients and constituent connections to forecast STS in MEP. Crossover, mutation, fitness measurement, and selection improve the formula. The empirical formula represents the complex concrete constituent—STS relationship mathematically. The following equation provides the mathematical equation for the STS model:

$$STS(MPa) = \frac{(CCA - 1)\sqrt{\sqrt{FA - CA + CG}}}{CD}$$

$$-\frac{\sqrt{2MC}}{CG - W + 1}$$

$$+\frac{CD}{(SHP - 1 + BFS)\sqrt{\sqrt{\sqrt{FA - CA + CG}}}},$$
(10)

where CCA denotes the corncob ash, SSG denotes the Na_2SiO_3 gel, BFS denotes the blast furnace slag, W denotes the water, SHP denotes the NaOH pellets, CG denotes the concrete grade, CA denotes the coarse aggregate, CD represents the curing day, MC represents the molar concentration, and FA represents the fine aggregate.

Figure 6(a) shows that the MEP model handles oversimplification and fresh, untested data well. Highly trained MEP models capture problem nuances through complicated data linkages. The model must manage oversimplification, over-fitting, and generalization to new data. In this equilibrium, the MEP model handles complexity without being too sophisticated to predict real-world outcomes. With an R^2 value similar to both the CS and FS-MEP models, the STS-MEP model appears to be a very accurate predictor of STS in SCA-GPC. As shown in Figure 6(b), MEP simulations investigate the absolute size of the gaps between the observed and desired values. Specifically, absolute differences show how far MEP predictions deviate from actual values on average. Lower absolute differences indicate a more accurate forecast, while larger differences indicate a wider error range, demonstrating the MEP model's dispersion and reliability. Predictions of MEP were within a range of 0.0033 to 0.440 MPa, according to the available data. There were 41 readings below 0.1 MPa, 36 values between 0.1 and 0.3 MPa, and 9 values over 0.3 MPa, resulting in an average error value lower than 0.136 MPa.

To avoid inaccuracies caused by differing scales, standardized unit measurements are used to guarantee that ML models consistently reflect input data. To reliably

Table 4: Results of statistical examination

Property			
	CS (MPa)	FS (MPa)	STS (MPa)
RSE	0.292	0.324	0.314
R	0.977	0.966	0.959
NSE	0.956	0.932	0.914
RMSE	2.347	0.265	0.173
MAE	1.79	0.199	0.136
RRMSE	0.614	0.556	0.628
MAPE	5.60	4.00	4.00

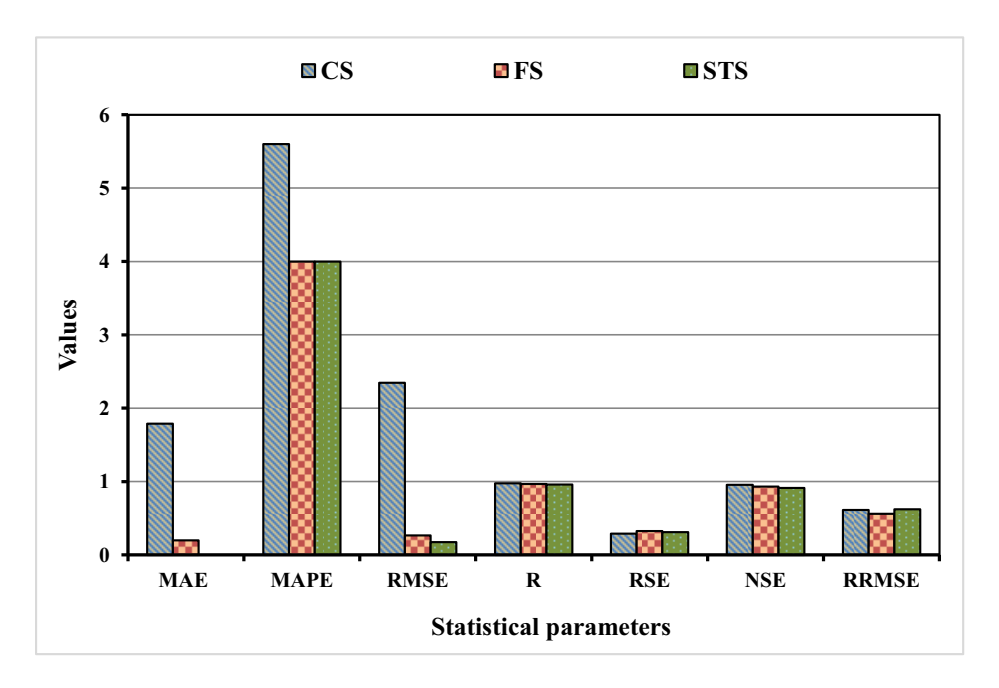


Figure 7: Statistical analysis of developed models.

compare the performance of models across various datasets, it is necessary to provide a consistent testing approach that guarantees uniform evaluation metrics. By offering a consistent framework for input representation and performance evaluation, these components improve the consistency and reliability of strength predictions in ML models. Inconsistent input representations and biases can result from changing or utilizing erroneous units in ML models. It may distort feature relevance, misinterpret relationships, and impair model generalization. Accurate and standardized units are

essential for model accuracy and meaningful comparisons across scenarios or datasets.

3.2 Authentication of MEP simulations

Table 4 shows the outcomes of the efficiency and error computations that were conducted using the aforementioned Eqs. (1) through (7): RSE, NSE, R, RMSE, RRMSE,

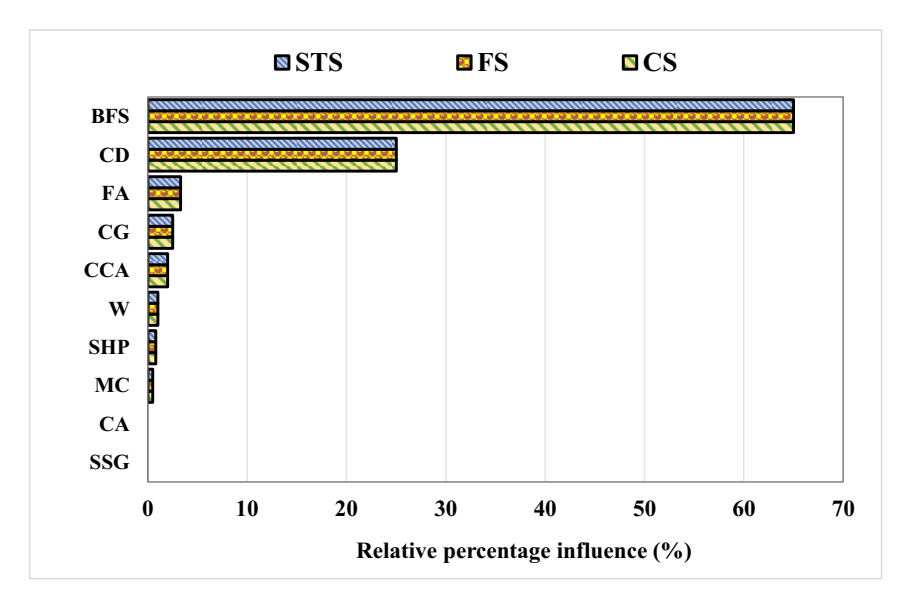


Figure 8: Sensitivity analysis for CS, FS, and STS outcomes.

14 — Jing Wang et al. DE GRUYTER

and MAE. The generated models have a higher level of accuracy in their predictions if their error values are smaller. The MEP models that relied on CS had an MAE of 1.79 MPa, FS had an MAE of 0.199 MPa, and STS had an MAE of 0.136 MPa. However, the MAPE values for the MEP models based on CS, FS, and STS were 5.60, 4.0, and 4.0, respectively. The other statistical errors, including RMSE, RSE, and RRMSE, also showed small values for the developed MEP models. The created models were evaluated not only for errors but also for efficiency, using two metrics: NSE and R. The greater the efficiency of a model, the more accurate its predictions will be. The MEP models based on CS, FS, and STS all had NSE values near 1 (0.956, 0.932, and 0.914, respectively), demonstrating the high quality of the MEP method's predictions. Similarities between the created models were revealed by the Pearson's coefficient (R). All of the statistical parameter-based forecasting models are compared in a bar chart (Figure 7). Among the most precise MLbased methods for predicting the mechanical characteristics of SCA-GPC, the MEP model stands out with its high R^2 , low error, excellent efficacy, and low average deviation.

3.3 Sensitivity analysis results

The focus of this research is on the effect of different input parameters on the SCA-GPC predictions of CS, FS, and STS. There is a strong correlation between the inputs and the outcomes that can be expected [87]. Figure 8 shows how each factor affects the mechanical properties of SCA-GPC, giving us a glimpse into the concrete of the future. BFS was the most influential factor (65%) among CS, FS, and STS; other factors that had a role were CD (25%), FA (3.30%), CG (2.50%), CCA (2.00%), water (1.00%), SHP (0.80%), and MC (0.50%). In contrast, the sensitivity analysis showed that SSG and CA had zero percent of an effect on the mechanical properties of SCA-GPC, indicating that there was very little variance in the dataset of parameters. The number of data points used in the sensitivity analysis was shown to be associated with the quantity of parameters used in the model. The study results changed based on the quantities of the concrete mix and other input parameters, which were initially hidden but became apparent upon implementing the ML technique. Input variables' relative importance was calculated using the following equations:

$$N_i = f_{\text{max}}(x_i) - f_{\text{min}}(x_i),$$
 (11)

$$S_i = \frac{N_i}{\sum_{i=i}^n N_i},\tag{12}$$



Figure 9: Benefits of producing and adopting waste-derived GPC in construction [90].

where $f_{\text{max}}(x_i)$ and $f_{\text{min}}(x_i)$ represent the highest and lowest predicted values over all *i*th outputs, respectively.

4 Discussions

Benefiting from operating within a limited range of 10 input parameters, the study's MEP model ensures that the projections are particular to SCA–GPC, which is a major plus. Since all of the models use a similar investigating protocol and uniform unit measurements, their strength projections are also consistent. The mathematical equations utilized in models greatly aid in comprehending the mix design and the impact of each input component. Though, the predicted models might not work if

Table 5: Previous modeling techniques used for GPC

Ref.	Technique	Input variables	Property	Best <i>R</i> ²- value
[88]	DNN, ResNet	9	CS	0.98
[20]	SVM, BPNN, ELM	14	CS	0.95
[87]	ANN, Boosting, AdaBoost	9	CS, FS	0.96
[89]	GEP, MEP	8	CS	0.97

parameters other than the ten inputs used are included in the overall evaluation. When fed data that is not what the models were built to handle, they may not function as intended. Incorrect or changed units of the input parameters might cause models to provide erroneous results. Maintaining constant unit sizes is critical to the model's performance. ML models have numerous uses in the construction industry, including predicting the strength of materials, ensuring quality, assessing risks, performing predictive maintenance, and improving energy efficiency. The requirement for human intervention, the existence of imprecise data, and the existence of erroneous models are just some of the constraints on these models. The Internet of Things, hybrid model development, explainable AI technique application, sustainability consideration, and industryspecific adjustments to data generation and distribution are all areas where these gaps might be filled and ML-based solutions enhanced by way of future studies. Reduced project duration and improved worker and environmental outcomes are possible effects of enhanced construction efficiency, interpretability, transparency, and data-driven decision-making. The results of this research could encourage more builders to use GPC, which would be a step toward more eco-friendly construction methods. Figure 9 displays the benefits of using GPC produced from waste in the building industry, whereas Table 5 offers the prior ML research conducted on GPC's various features with R^2 -values, suggesting the current study's comparable performance.

5 Limitations and recommendations for future research

CS, flexural strength, and split tensile strength were predicted using 260 data records in the current investigation. These forecasts were created after taking ten variables into account. Adding more records of data from experimental investigations could be a focus of future studies to further increase the models' accuracy. Predictions made by the model can be made more confidently and accurately by increasing the size of the dataset. In addition, MEP models were used in this investigation. However, future studies could investigate the use of hybrid ML techniques such as the genetic algorithm with particle swarm optimization and the RF-ANN, as well as individual/standalone and ensemble algorithms such as the SVM, DT, bagging, and boosting. These hybrid methods have the potential to significantly improve the models' performance and prediction capacities; therefore, it makes sense to incorporate them. There are additional post hoc explanatory techniques that can be used to shed light on the ML model's prediction, such as the SHapley Additive exPlanations technique, Local Interpretable Model-Agnostic Explanations, and Partial Dependence Plots, which were not used in this study but are available. Most of the available literature on using ML techniques to predict the properties of GPC focuses on mechanical properties. Nonetheless, there is a clear lack of studies looking at the GPC's durability, dynamic attributes (fatigue), and microstructure. More research is needed to use ML techniques to investigate these durability factors in depth.

6 Conclusions

This study developed mechanical property prediction models for slag-CCA GPC (SCA-GPC) using MEP. The models were trained and verified using 260 sets of mechanical characteristics data, including compressive, flexural, and split tensile strengths. The study's main findings are as follows:

The study concluded that MEP models performed exceptionally in terms of data prediction accuracy in forecasting the mechanical strength of SCA-GPC.

For SCA-GPC's mechanical properties prediction, CS-MEP, FS-MEP, and STS-MEP models achieved R^2 values above 0.90, which exhibits that MEP models agreed well with the actual findings.

The effectiveness of the developed models was assessed using statistical performance measures (MAE, RMSE, MAPE, R, RSE, NSE, and RRMSE). Lower errors and higher R indicate ML model accuracy. Error rates and R results supported the claim that MEP models accurately predicted SCA-GPC mechanical properties.

According to the sensitivity analysis, BFS (65%), CD (25%), and FA (3.30%) were the key input parameters with a higher impact on the mechanical properties of SCA-GPC.

MEP's significance lies in the fact that it offers a one-ofa-kind mathematical formula that can be applied to the prediction of features in another database. The mathematical models resulting from this study can help scientists and engineers rapidly assess, enhance, and rationalize GPC mixture proportioning.

Acknowledgments: The authors are thankful to the Deanship of Scientific Research at Najran University for funding this work, under the Research Groups Funding program (Grant Code: NU/RG/SERC/12/1).

Funding information: This article was sponsored by the 2021 Chongqing Vocational and Technical College of Industry's New Product and New Technology Special Project "Research on the Preparation of High Strength Concrete Mix Proportion by Microbial Deposited Calcium Carbonate Reinforced Recycled Fine Aggregate" (GZY2021-NEW-06).

Author contributions: J.W.: conceptualization, funding acquisition, project administration, supervision, writing-original draft. Q.Q.: data acquisition, conceptualization, formal analysis, methodology, writing, reviewing, and editing. S.A.K.: investigation, software, supervision, writing-original draft, writing, reviewing, and editing. B.S.A.: formal analysis, resources, writing, reviewing, and editing. F.A: conceptualization, visualization, writing, reviewing, and editing. Y.G.: investigation, validation, writing, reviewing, and editing. T.N. funding acquisition, data acquisition, writing, reviewing, and editing. All authors have accepted responsibility for the entire content of this manuscript and approved its submission.

Conflict of interest: The authors state no conflict of interest.

Data availability statement: The datasets generated during and/or analyzed during the current study are available from the corresponding author upon a reasonable request.

References

- [1] Ghosh, A. and G. D. Ransinchung. Application of machine learning algorithm to assess the efficacy of varying industrial wastes and curing methods on strength development of geopolymer concrete. Construction and Building Materials, Vol. 341, 2022, id. 127828.
- [2] Belaïd, F. How does concrete and cement industry transformation contribute to mitigating climate change challenges? Resources. Conservation & Recycling Advances, Vol. 15, 2022, id. 200084.
- [3] Andrew, R. M. Global CO 2 emissions from cement production, 1928–2018. Earth System Science Data, Vol. 11, 2019, pp. 1675–1710.
- [4] Puertas, F., J. A. Suárez-Navarro, M. M. Alonso, and C. Gascó. NORM waste, cements, and concretes. A review, *Materiales de Construcción*, Vol. 71, No. 344, 2021, id. e259.
- [5] Xiao, R., B. Huang, H. Zhou, Y. Ma, and X. Jiang. A state-of-the-art review of crushed urban waste glass used in OPC and AAMs (geopolymer): Progress and challenges. *Cleaner Materials*, Vol. 4, 2022. id. 100083.
- [6] Shilar, F. A., S. V. Ganachari, V. B. Patil, B. E. Bhojaraja, T. M. Y. Khan, and N. Almakayeel. A review of 3D printing of geopolymer composites for structural and functional applications. *Construction and Building Materials*, Vol. 400, 2023, id. 132869.
- [7] Elmagarhe, A., Q. Lu, M. Alharthai, M. Alamri, and A. Elnihum. Performance of porous asphalt mixtures containing recycled concrete aggregate and fly ash. *Materials*, Vol. 15, 2022, id. 6363.

- [8] Schaubroeck, T., T. Gibon, E. Igos, and E. Benetto. Sustainability assessment of circular economy over time: Modelling of finite and variable loops & impact distribution among related products. Resources, Conservation and Recycling, Vol. 168, 2021, id. 105319.
- [9] Shilar, F. A., S. V. Ganachari, V. B. Patil, N. Almakayeel, and T. M. Y. Khan. Development and optimization of an eco-friendly geopolymer brick production process for sustainable masonry construction. Case Studies in Construction Materials, Vol. 18, 2023, id. e02133.
- [10] Shaaban, I. G., J. P. Rizzuto, A. El-Nemr, L. Bohan, H. Ahmed, and H. Tindyebwa. Mechanical properties and air permeability of concrete containing waste tires extracts. *Journal of Materials in Civil Engineering*, Vol. 33, 2021, id. 04020472.
- [11] Nurruddin, M. F., H. Sani, B. S. Mohammed, and I. Shaaban. Methods of curing geopolymer concrete: A review. *International Journal of Advanced and Applied Sciences*, Vol. 5, 2018, pp. 31–36.
- [12] Saif, M. S., A. S. Shanour, G. E. Abdelaziz, H. I. Elsayad, I. G. Shaaban, B. A. Tayeh, et al. Influence of blended powders on properties of ultra-high strength fibre reinforced self compacting concrete subjected to elevated temperatures. *Case Studies in Construction Materials*, Vol. 18, 2023, id. e01793.
- [13] Oyebisi, S., A. Ede, F. Olutoge, and D. Omole. Geopolymer concrete incorporating agro-industrial wastes: Effects on mechanical properties, microstructural behaviour and mineralogical phases.

 Construction and Building Materials, Vol. 256, 2020, id. 119390.
- [14] Oyebisi, S., A. Ede, F. Olutoge, and B. Ngene. Assessment of activity indexes on the splitting tensile strengthening of geopolymer concrete incorporating supplementary cementitious materials. *Materials Today Communications*, Vol. 24, 2020, id. 101356.
- [15] Sarah Kareem Mohammed, A.-S., R. Géber, A. Simon, E. Kurovics, and A. Hamza. Comparative study of metakaolin-based geopolymer characteristics utilizing different dosages of water glass in the activator solution. *Results in Engineering*, Vol. 20, 2023, id. 101469.
- [16] Davidovits, J. Geopolymers: Inorganic polymeric new materials. Journal of Thermal Analysis and Calorimetry, Vol. 37, 1991, pp. 1633–1656.
- [17] Khale, D. and R. Chaudhary. Mechanism of geopolymerization and factors influencing its development: a review. *Journal of Materials Science*, Vol. 42, 2007, pp. 729–746.
- [18] Pazouki, G. Fly ash-based geopolymer concrete's compressive strength estimation by applying artificial intelligence methods. *Measurement*, Vol. 203, 2022. jd. 111916.
- [19] He, J., Y. Jie, J. Zhang, Y. Yu, and G. Zhang. Synthesis and characterization of red mud and rice husk ash-based geopolymer composites. *Cement and Concrete Composites*, Vol. 37, 2013, pp. 108–118.
- [20] Peng, Y. and C. Unluer. Analyzing the mechanical performance of fly ash-based geopolymer concrete with different machine learning techniques. *Construction and Building Materials*, Vol. 316, 2022, id. 125785.
- [21] Shahmansouri, A. A., M. Yazdani, S. Ghanbari, H. A. Bengar, A. Jafari, and H. F. Ghatte. Artificial neural network model to predict the compressive strength of eco-friendly geopolymer concrete incorporating silica fume and natural zeolite. *Journal of Cleaner Production*, Vol. 279, 2021, id. 123697.
- [22] Zhang, C., Z. Zhu, F. Liu, Y. Yang, Y. Wan, W. Huo, et al. Efficient machine learning method for evaluating compressive strength of cement stabilized soft soil. *Construction and Building Materials*, Vol. 392, 2023, id. 131887.
- [23] Singh, B., G. Ishwarya, M. Gupta, and S. K. Bhattacharyya. Geopolymer concrete: A review of some recent developments. *Construction and Building Materials*, Vol. 85, 2015, pp. 78–90.

- [24] Xiao, R., X. Jiang, M. Zhang, P. Polaczyk, and B. Huang. Analytical investigation of phase assemblages of alkali-activated materials in CaO-SiO2-Al2O3 systems: The management of reaction products and designing of precursors. Materials & Design, Vol. 194, 2020, id. 108975.
- [25] Xiao, R., Z. Shen, R. Si, P. Polaczyk, Y. Li, H. Zhou, et al. Alkaliactivated slag (AAS) and OPC-based composites containing crumb rubber aggregate: Physico-mechanical properties, durability and oxidation of rubber upon NaOH treatment. Journal of Cleaner Production, Vol. 367, 2022, id. 132896.
- [26] Shilar, F. A., S. V. Ganachari, V. B. Patil, I. N. Reddy, and J. Shim. Preparation and validation of sustainable metakaolin based geopolymer concrete for structural application. Construction and Buildina Materials, Vol. 371, 2023, id. 130688.
- [27] Shilar, F. A., S. V. Ganachari, V. B. Patil, S. Javed, T. M. Y. Khan, and R. U. Baig. Assessment of destructive and nondestructive analysis for GGBS based geopolymer concrete and its statistical analysis. Polymers, Vol. 14, 2022, id. 3132.
- [28] Lenka, B. P., R. K. Majhi, S. Singh, and A. N. Nayak. Eco-friendly and cost-effective concrete utilizing high-volume blast furnace slag and demolition waste with lime. European Journal of Environmental and Civil Engineering, Vol. 26, 2022, pp. 5351-5373.
- [29] Majhi, R. K. and A. N. Nayak. Production of sustainable concrete utilising high-volume blast furnace slag and recycled aggregate with lime activator. Journal of Cleaner Production, Vol. 255, 2020, id.
- [30] Revilla-Cuesta, V., V. Ortega-López, M. Skaf, and J. M. Manso. Deformational behavior of self-compacting concrete containing recycled aggregate, slag cement and green powders under compression and bending: Description and prediction adjustment. Journal of Building Engineering, Vol. 54, 2022, id. 104611.
- [31] Ortega-López, V., F. Faleschini, C. Pellegrino, V. Revilla-Cuesta, and J. M. Manso. Validation of slag-binder fiber-reinforced self-compacting concrete with slag aggregate under field conditions: Durability and real strength development. Construction and Building Materials, Vol. 320, 2022, id. 126280.
- [32] Majhi, R. K., A. N. Nayak, and B. B. Mukharjee. Characterization of lime activated recycled aggregate concrete with high-volume ground granulated blast furnace slag. Construction and Building Materials, Vol. 259, 2020, id. 119882.
- [33] Xiao, R., Q. Nie, J. He, H. Lu, Z. Shen, and B. Huang. Utilizing lowlyreactive coal gasification fly ash (CGFA) to stabilize aggregate bases. Journal of Cleaner Production, Vol. 370, 2022, id. 133320.
- [34] Perera, S. T. A. M., J. Zhu, M. Saberian, M. Liu, D. Cameron, T. Magsood, et al. Application of glass in subsurface pavement layers: A comprehensive review. Sustainability, Vol. 13, 2021, id. 11825.
- [35] Zakka, W. P., N. H. A. S. Lim, and M. C. Khun. A scientometric review of geopolymer concrete. Journal of Cleaner Production, Vol. 280, 2021, id. 124353.
- [36] Farooq, F., X. Jin, M. F. Javed, A. Akbar, M. I. Shah, F. Aslam, et al. Geopolymer concrete as sustainable material: A state of the art review. Construction and Building Materials, Vol. 306, 2021, id.
- [37] Ahmed, H. U., A. A. Mohammed, and A. S. Mohammed. Effectiveness of silicon dioxide nanoparticles (Nano SiO2) on the internal structures, electrical conductivity, and elevated temperature behaviors of geopolymer concrete composites. Journal of Inorganic and Organometallic Polymers and Materials, Vol. 33, 2023, pp. 1-21.

- [38] Ahmed, H. U., A. S. Mohammed, and A. A. Mohammed. Engineering properties of geopolymer concrete composites incorporated recycled plastic aggregates modified with nano-silica. Journal of Building Engineering, Vol. 75, 2023, id. 106942.
- Ahmed, H. U., A. A. Mohammed, and A. S. Mohammed. Effectiveness of nano-SiO2 on the mechanical, durability, and microstructural behavior of geopolymer concrete at different curing ages. Archives of Civil and Mechanical Engineering, Vol. 23, 2023, pp. 1-28.
- [40] Avci, O., O. Abdeljaber, S. Kiranyaz, M. Hussein, M. Gabbouj, and D. J. Inman. A review of vibration-based damage detection in civil structures: From traditional methods to Machine Learning and Deep Learning applications. Mechanical Systems and Signal Processing, Vol. 147, 2021, id. 107077.
- Ghahramani, Z. Probabilistic machine learning and artificial intelligence. Nature, Vol. 521, 2015, pp. 452-459.
- [42] Stocker, T. Climate change 2013: The physical science basis: Working Group I contribution to the Fifth assessment report of the Intergovernmental Panel on Climate Change, Cambridge University Press, New York, USA, 2014.
- [43] Dietterich, T. G. Ensemble methods in machine learning, In: Multiple Classifier Systems. MCS 2000. Lecture Notes in Computer Science, Vol. 1857. Springer, Berlin, Heidelberg, 2000, pp. 1-15.
- [44] Haenlein, M. and A. Kaplan. A brief history of artificial intelligence: On the past, present, and future of artificial intelligence. California Management Review, Vol. 61, 2019, pp. 5-14.
- Marani, A. and M. L. Nehdi. Machine learning prediction of compressive strength for phase change materials integrated cementitious composites. Construction and Building Materials, Vol. 265, 2020, id. 120286.
- [46] Ahmad, A., W. Ahmad, F. Aslam, and P. Joyklad. Compressive strength prediction of fly ash-based geopolymer concrete via advanced machine learning techniques. Case Studies in Construction Materials, Vol. 16, 2022, id. e00840.
- [47] Oyebisi, S. and T. Alomayri. Artificial intelligence-based prediction of strengths of slag-ash-based geopolymer concrete using deep neural networks. Construction and Building Materials, Vol. 400, 2023,
- [48] Timur Cihan, M. Prediction of concrete compressive strength and slump by machine learning methods. Advances in Civil Engineering, Vol. 2019, 2019, pp. 1-11.
- [49] Raza A., Q. u. Z. Khan, and A. Ahmad. Prediction of axial compressive strength for FRP-confined concrete compression members. KSCE Journal of Civil Engineering, Vol. 24, 2020, pp. 2099-2109.
- [50] Mansour, M. Y., M. Dicleli, J.-Y. Lee, and J. Zhang. Predicting the shear strength of reinforced concrete beams using artificial neural networks. Engineering Structures, Vol. 26, 2004, pp. 781-799.
- [51] Tamimi, A. K., J. A. Abdalla, and Z. I. Sakka. Prediction of long term chloride diffusion of concrete in harsh environment. Construction and Building Materials, Vol. 22, 2008, pp. 829-836.
- [52] Nazar, S., J. Yang, A. Ahmad, and S. F. A. Shah. Comparative study of evolutionary artificial intelligence approaches to predict the rheological properties of fresh concrete. Materials Today Communications, Vol. 32, 2022, id. 103964.
- [53] Song, H., A. Ahmad, F. Farooq, K. A. Ostrowski, M. Maślak, S. Czarnecki, et al. Predicting the compressive strength of concrete with fly ash admixture using machine learning algorithms. Construction and Building Materials, Vol. 308, 2021, id. 125021.

- [54] Moein, M. M., A. Saradar, K. Rahmati, S. H. G. Mousavinejad, J. Bristow, V. Aramali, et al. Predictive models for concrete properties using machine learning and deep learning approaches: A review. *Journal of Building Engineering*, Vol. 63, 2022, id. 105444.
- [55] Khan, K., M. N. Amin, U. U. Sahar, W. Ahmad, K. Shah, and A. Mohamed. Machine learning techniques to evaluate the ultrasonic pulse velocity of hybrid fiber-reinforced concrete modified with nano-silica. *Frontiers in Materials*, Vol. 9, 2022, id. 1098304.
- [56] Kabiru, O. A., T. O. Owolabi, T. Ssennoga, and S. O. Olatunji. Performance comparison of SVM and ANN in predicting compressive strength of concrete. *IOSR Journal of Computer Engineering (IOSR-JCE)*, Vol. 16, 2014, pp. 88–94.
- [57] Raheem, A., B. Ikotun, S. Oyebisi, and A. Ede. Machine learning algorithms in wood ash-cement-Nano TiO2-based mortar subjected to elevated temperatures. *Results in Engineering*, Vol. 18, 2023, id. 101077.
- [58] Saaidi, A., A. Bichri, and S. Abderafi. Efficient machine learning model to predict dynamic viscosity in phosphoric acid production. *Results in Engineering*, Vol. 18, 2023, id. 101024.
- [59] Mermerdas, K., S. M. Oleiwi, and S. R. Abid. Modeling compressive strength of lightweight geopolymer mortars by step-wise regression and gene expression programming. *Hittite Journal of Science* and Engineering, Vol. 6, 2019, pp. 157–166.
- [60] Faraz, M. I., S. U. Arifeen, M. N. Amin, A. Nafees, F. Althoey, and A. Niaz. A comprehensive GEP and MEP analysis of a cement-based concrete containing metakaolin. *Structures*, Vol. 53, 2023, pp. 937–948.
- [61] Li, Z., S. Bao, X. Xu, Y. Bao, and Y. Zhang. Polymorphisms of CHRNA5-CHRNA3-CHRNB4 gene cluster and NSCLC risk in Chinese population. *Translational Oncology*, Vol. 5, 2012, pp. 448–452.
- [62] Khan, M. A., F. Farooq, M. F. Javed, A. Zafar, K. A. Ostrowski, F. Aslam, et al. Simulation of depth of wear of eco-friendly concrete using machine learning based computational approaches. *Materials*, Vol. 15, 2021, id. 58.
- [63] Amin, M. N., S. A. Khan, K. Khan, S. Nazar, A. M. A. Arab, and A. F. Deifalla. Promoting the suitability of rice husk ash concrete in the building sector via contemporary machine intelligence techniques. Case Studies in Construction Materials, Vol. 19, 2023, id. e02357.
- [64] Cao, Q., X. Yuan, M. Nasir Amin, W. Ahmad, F. Althoey, and F. Alsharari. A soft-computing-based modeling approach for predicting acid resistance of waste-derived cementitious composites. Construction and Building Materials, Vol. 407, 2023, id. 133540.
- [65] Chen, Z., M. N. Amin, B. Iftikhar, W. Ahmad, F. Althoey, and F. Alsharari. Predictive modelling for the acid resistance of cement-based composites modified with eggshell and glass waste for sustainable and resilient building materials. *Journal of Building Engineering*, Vol. 76, 2023, id. 107325.
- [66] Khan, K., W. Ahmad, M. N. Amin, and A. F. Deifalla. Investigating the feasibility of using waste eggshells in cement-based materials for sustainable construction. *Journal of Materials Research and Technology*, Vol. 23, 2023, pp. 4059–4074.
- [67] Lee, B. C. and D. M. Brooks. Accurate and efficient regression modeling for microarchitectural performance and power prediction. ACM SIGOPS Operating Systems Review, Vol. 40, 2006, pp. 185–194.
- [68] Wang, H.-L. and Z.-Y. Yin. High performance prediction of soil compaction parameters using multi expression programming. *Engineering Geology*, Vol. 276, 2020, id. 105758.
- [69] Iqbal, M. F., M. F. Javed, M. Rauf, I. Azim, M. Ashraf, J. Yang, et al. Sustainable utilization of foundry waste: Forecasting mechanical properties of foundry sand based concrete using multi-expression

- programming. Science of the Total Environment, Vol. 780, 2021, id. 146524.
- [70] Oltean, M. and C. Grosan. A comparison of several linear genetic programming techniques. *Complex Systems*, Vol. 14, 2003, pp. 285–314.
- [71] Fallahpour, A., E. U. Olugu, and S. N. Musa. A hybrid model for supplier selection: integration of AHP and multi expression programming (MEP). *Neural Computing and Applications*, Vol. 28, 2017, pp. 499–504.
- [72] Alavi, A. H., A. H. Gandomi, M. G. Sahab, and M. Gandomi. Multi expression programming: a new approach to formulation of soil classification. *Engineering with Computers*, Vol. 26, 2010, pp. 111–118.
- [73] Mohammadzadeh S, D., S.-F. Kazemi, A. Mosavi, E. Nasseralshariati, and J. H. M. Tah. Prediction of compression index of fine-grained soils using a gene expression programming model. *Infrastructures*, Vol. 4, 2019, id. 26.
- [74] Grosan, C., and A. Abraham. Stock market modeling using genetic programming ensembles. In *Genetic systems programming: Theory* and experiences, Springer, Berlin, Germany, 2006, p. 131–146.
- [75] Oltean, M. and D. Dumitrescu. Multi expression programming. Journal of Genetic Programming and Evolvable Machines, 2002.
- [76] Amin, M. N., W. Ahmad, K. Khan, and A. F. Deifalla. Optimizing compressive strength prediction models for rice husk ash concrete with evolutionary machine intelligence techniques. Case Studies in Construction Materials, Vol. 18, 2023, id. e02102.
- [77] Iqbal, M. F., Q.-f Liu, I. Azim, X. Zhu, J. Yang, M. F. Javed, et al. Prediction of mechanical properties of green concrete incorporating waste foundry sand based on gene expression programming. *Journal of Hazardous Materials*, Vol. 384, 2020, id. 121322.
- [78] Shahin, M. A. Genetic programming for modelling of geotechnical engineering systems, Springer, 2015.
- [79] Çanakcı, H., A. Baykasoğlu, and H. Güllü. Prediction of compressive and tensile strength of Gaziantep basalts via neural networks and gene expression programming. *Neural Computing and Applications*, Vol. 18, 2009, pp. 1031–1041.
- [80] Alade, I. O., M. A. Abd Rahman, and T. A. Saleh. Predicting the specific heat capacity of alumina/ethylene glycol nanofluids using support vector regression model optimized with Bayesian algorithm. Solar Energy, Vol. 183, 2019, pp. 74–82.
- [81] Alade, I. O., A. Bagudu, T. A. Oyehan, M. A. Abd Rahman, T. A. Saleh, and S. O. Olatunji. Estimating the refractive index of oxygenated and deoxygenated hemoglobin using genetic algorithm–support vector regression model. *Computer Methods and Programs in Biomedicine*, Vol. 163, 2018, pp. 135–142.
- [82] Zhang, W., R. Zhang, C. Wu, A. T. C. Goh, S. Lacasse, Z. Liu, et al. State-of-the-art review of soft computing applications in underground excavations. *Geoscience Frontiers*, Vol. 11, 2020, pp. 1095–1106.
- [83] Alavi, A. H., A. H. Gandomi, H. C. Nejad, A. Mollahasani, and A. Rashed. Design equations for prediction of pressuremeter soil deformation moduli utilizing expression programming systems. Neural Computing and Applications, Vol. 23, 2013, pp. 1771–1786.
- [84] Kisi, O., J. Shiri, and M. Tombul. Modeling rainfall-runoff process using soft computing techniques. *Computers & Geosciences*, Vol. 51, 2013, pp. 108–117.
- [85] Alade, I. O., M. A. Abd Rahman, and T. A. Saleh. Modeling and prediction of the specific heat capacity of Al2 O3/water nanofluids using hybrid genetic algorithm/support vector regression model. Nano-Structures & Nano-Objects, Vol. 17, 2019, pp. 103–111.

- [86] Shahin, M. A. Use of evolutionary computing for modelling some complex problems in geotechnical engineering. Geomechanics and Geoengineering, Vol. 10, 2015, pp. 109-125.
- [87] Ahmad, A., W. Ahmad, K. Chaiyasarn, K. A. Ostrowski, F. Aslam, P. Zajdel, et al. Prediction of geopolymer concrete compressive strength using novel machine learning algorithms. Polymers, Vol. 13, 2021, id. 3389.
- [88] Nguyen, K. T., Q. D. Nguyen, T. A. Le, J. Shin, and K. Lee. Analyzing the compressive strength of green fly ash based geopolymer concrete using experiment and machine learning approaches. Construction and Building Materials, Vol. 247, 2020, id. 118581.
- [89] Chu, H.-H., M. A. Khan, M. Javed, A. Zafar, M. I. Khan, H. Alabduljabbar, et al. Sustainable use of fly-ash: Use of geneexpression programming (GEP) and multi-expression programming (MEP) for forecasting the compressive strength geopolymer concrete. Ain Shams Engineering Journal, Vol. 12, 2021, pp. 3603-3617.
- [90] Yang, H., L. Liu, W. Yang, H. Liu, W. Ahmad, A. Ahmad, et al. A comprehensive overview of geopolymer composites: A bibliometric analysis and literature review. Case Studies in Construction Materials, Vol. 16, 2022, id. e00830.